IMPROVING VERTICAL AND LATERAL RESOLUTION BY STRETCH-FREE, HORIZON-ORIENTED IMAGING

Gabriel Pérez[1] and Kurt Marfurt[2]

(1) Gabriel Pérez: Geosciences department. University of Houston. Houston, Texas 77204-5007. Geophysics Ph.D Research Assistant. gabriel.perez@mail.uh.edu

(2) Kurt Marfurt: Geosciences department. Professor, Director of AGL. University of Houston. Houston, Texas 77204-5007. kmarfurt@uh.edu

ABSTRACT

The pre-stack Kirchhoff migration is implemented for delivering wavelet stretch-free imaged data, if the migration is (ideally) limited to the wavelet corresponding to a target horizon. Avoiding wavelet stretch provides long-offset imaged data, far beyond what is reached in conventional migration and results in images from the target with improved vertical and lateral resolution and angular illumination. Increasing the range of imaged offsets also increases the sensitivity to event-crossing, velocity errors and anisotropy. These issues must be addressed to fully achieve the greatest potential of this technique. These ideas are further illustrated with a land survey seismic data application in Texas, U.S.

Keywords: Pre-stack Kirchoff migration, seimic data, wavelet stretch-free data, Texas.

RESUMEN

La migración de pre-apilamiento de Kirchhoff proporciona imágenes que no sufren de estiramiento de la ondícula, si la migración es (idealmente) limitada a la ondícula correspondiente al horizonte de interés. Al evitar el estiramiento de la ondícula se pueden generar imágenes a partir de datos con separación grande entre fuente y receptor, mas allá de lo que se puede alcanzar con la migración convencional y se logran imágenes del objetivo con mejor resolución vertical y horizontal y mejor iluminación angular. Al aumentar el rango aceptable de separación entre fuente y receptor, también incrementa la sensibilidad al cruce entre eventos, errores de velocidad y anisotropía. Para obtener los mejores resultados con esta técnica, estos factores deben ser tratados adecuadamente. Para ilustrar estas ideas, presentamos una aplicación a datos sísmicos 3D adquiridos en Texas, US.

Palabras Clave: Pre-stack Kirchoff migration, seimic data, wavelet stretch-free data, Texas.

INTRODUCTION

Surface seismic data are a major source of information about the subsurface. Roughly, this comes in two different ways: through seismic images that illuminate structure and stratigraphy, and from the study of data attributes such as amplitude, arrival time or frequency content that are sensitive to lithology and fluid content. Exploration challenges steadily place increasing demands on all factors that impact the usefulness and quality of this information such as frequency content and availability of long-offset data. Increasing frequency content is desired to achieve the level of lateral and vertical resolution required for even smaller and/or more elusive targets. Increasing the usable range of offsets in the data is desired to support AVO studies, anisotropy and velocity analysis, or simply to increase the fold of stacking. Unfortunately, these two factors are sometimes counteracting in common seismic exploration practice.

Specifically, when it comes to imaging, either in conventional NMO or in pre-stack migration, loss of frequency content and wavelet distortion due to stretch is a major problem for far-offset data. Typically, imaged data beyond a certain offset, roughly between once to twice the reflection depth, is severely distorted due to stretch that it needs to be discarded by harsh muting. While several methods have been proposed to alleviate NMO stretch (Dunkin and Levin, 1973; Rupert and Chun, 1975; Barnes, 1992), little attention has been devoted to stretch due to migration. In addition, recent approaches attack the problem during the stacking process, thereby resulting in an improved stacked image but not delivering stretch-free pre-stack traces (Trickett, 2003). In that case, an increased fold of stack but none of the other desired benefits mentioned above is achieved. Recently, wavelet stretch has been recognized as a major adverse factor in AVO (Swan, 1997; Dong, 1999) and increasing attention has been given to develop methods to quantify and correct for its effects. Though most approaches focus on the improved estimation of attributes such as AVO intercept and gradient or 3-term AVO/AVA inversion, some directly or indirectly attempt to correct for stretch on the data itself (Shatilo and Aminzadeh, 2000; Castoro et al, 2001; Brouwer, 2002; Lazaratos and Finn, 2004).

Hilterman and VanSchuyver (2003), working in long offset AVO, introduced a horizon-oriented pre-stack migration implementation that generates stretch-free pre-stack imaged data. Besides from the AVO focus, the impact of such horizon-oriented stretch-free prestack imaging and the availability of long-offset stretch-free imaged data on image quality and lateral and vertical seismic resolution will be explored, through data from a land survey application in Texas, U.S. The impact of such imaging on a land seismic dataset is assessed through the use of multitrace geometric seismic attributes. The attributes computed from pre-stack seismic data may reveal subtle geologic features that are lost in conventional stacked images. In the interest of maximizing the science with a reasonable computational effort, pre-stack time migration has been used as the preferred imaging method.

HORIZON-ORIENTED STRETCH-FREE PRESTACK IMAGING

As discussed by Levin (1998), wavelet stretch occurs in all pre-stack imaging methods. Within the context of Kirchhoff migration, this stretch is associated to the variation in the curvature of isochron surfaces for different times on an input seismic trace (Figure 1). Using the analogy of Kirchhoff migration as a moving operation, if "migration paths were somehow parallel", stretch would be avoided. As suggested in Figure 2, it would be possible to "move" a block of input samples along a single path. In this way, relative separation within the samples in the block is not altered so no stretch is introduced. This idea can be actually implemented in practice by computing a traveltime operator that is exact for a single output position and then, migrating a window of the data centered on the computed arrival time, instead of migrating just the single sample matching that time. The central sample is migrated to the "exact" position in the output and, for time migration; surrounding samples are migrated to positions in which the difference in time with respect to the central migrated sample are preserved. In depth migration, a similar outcome can be achieved by scaling the time differences
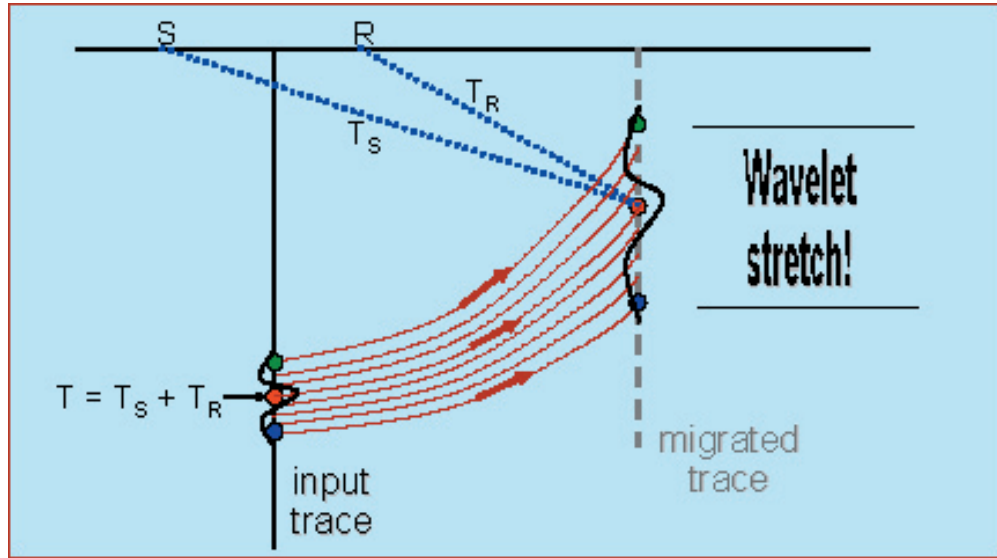
Figure. 1. Kirchhoff migration schematics and its action on a band-limited wavelet. The data sample whose timing matches the total traveltime from source location to subsurface position and back to receiver location, with proper scaling, is the contribution from the input trace to the image at the given position. In time migration, if the timing within the samples in the wavelet is changed in the output, relative to the input, the wavelet will be distorted accordingly. In depth migration, variations in the separation between output samples, assuming uniform sampling in time in the input data, will also result on differential stretch or squeeze on the wavelet.
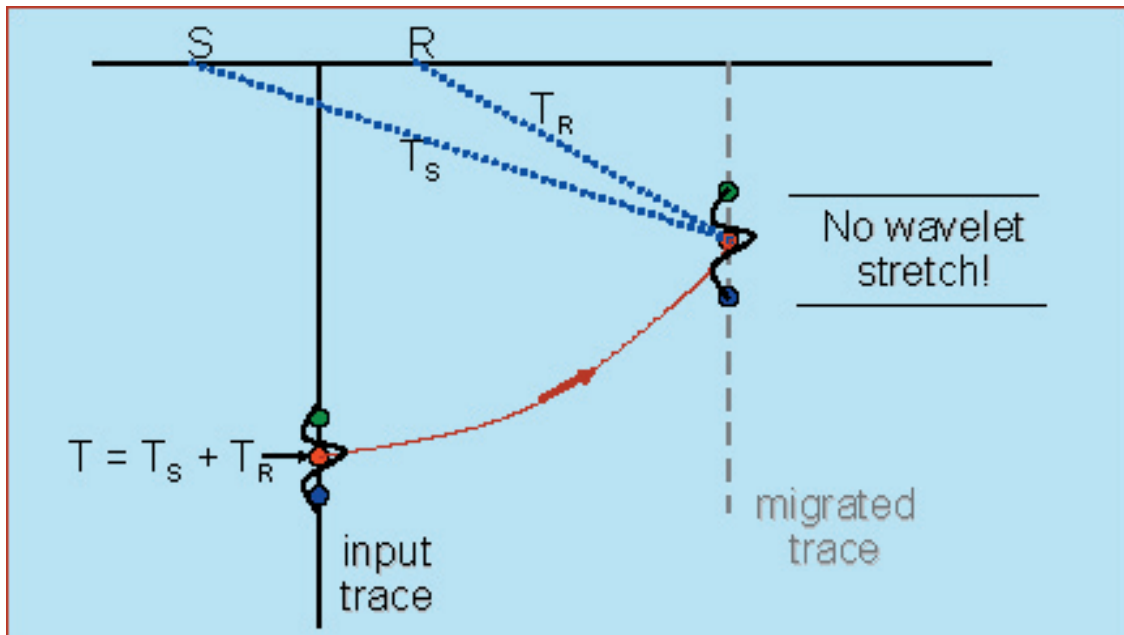

Figure. 2. Instead of "moving" individual samples independently, a block of samples is moved along "parallel" paths so that relative separation between samples is not altered, hence no stretch is introduced. Ideally the block of samples should include the wavelet associated to the event of interest. This is a modification of the operation shown in Figure 1.
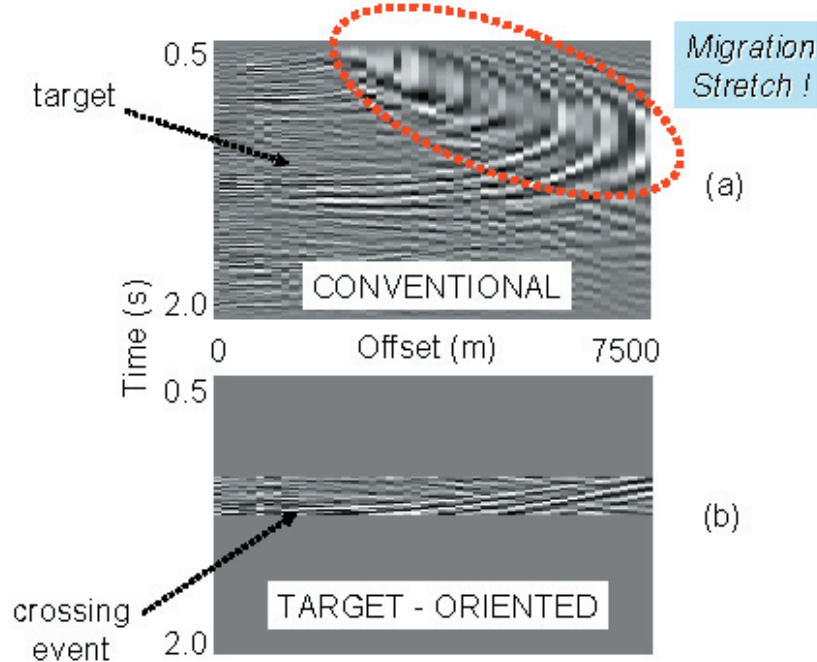
Figure. 3. Comparison of imaged gathers pertaining to the same image location, for the: (a) conventional and (b) target-oriented migrations. Notice that, by contrast with the conventional migration, the target-oriented migrated data is stretch-free. The event used as a target for the target-oriented migration is shown in blue in both panels. As depicted by the dotted blue line, the desired definition of this event in the longest offsets in the target-oriented migration is obscured by interference from crossing events such as the one marked in yellow. The inferred location of this event on the conventional migrated data is shown with a broken line.

by a factor given by the local value of the migration velocity. This simply amounts to conversion from uniform sampling in time to uniform sampling in depth with scaling given by that factor (see Yu et al., 2004 for an application of this idea to wavelet-based depth migration).

Notice that samples other than the central matching sample are not migrated properly, that is, to the position they would be migrated in conventional migration. In that regard, this approach is only accurate locally, at most in a relatively narrow window around the central matching sample, where the error introduced is small. In the other hand, the migration operation just described makes perfect sense if the matching sample corresponds to a reflector, and instead of just a block of samples operating over the wavelet corresponding to the reflector is considered. In that case, the wavelet is simply kept (with proper scaling to depth, in the case of depth migration) attached to the image of the reflector that carries it. The whole operation amounts to the

migration of a broad-band impulse representing the reflector, followed by convolution with the wavelet. Using a block of samples is simply a practical way of avoiding the added complication of determination of the wavelet; the size of the block has to be large enough to include the wavelet. Regardless of which of the two points of view just discussed is preferred, it is clear that the imaging approach described is limited, because of either accuracy or scope, to a relatively narrow window around a previously chosen target horizon or target depth. Because of this, the migration is limited to a narrow window of input trace samples (usually within 50ms to 200 ms thick) surrounding the originally selected time.

Similar methods have been developed elsewhere. Wyatt et al. (1997) describe an application with emphasis on the efficiency in computation and human intervention provided by imaging limited to a narrow zone around a horizon. Our interest arises from the work of Hilterman (2004) on improving the frequency content of long-off-
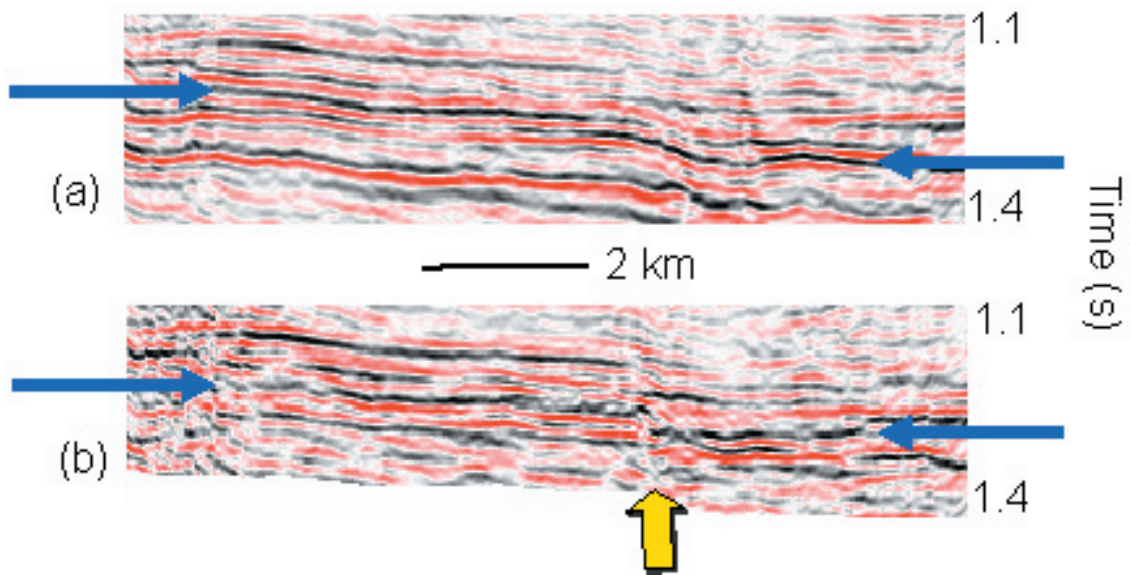
150

Figure. 4. Comparison between images for a selected inline from the 3D volume for the: (a) conventional and (b) target oriented migrations. Images stacked over the full range of offsets available to each migration. The blue arrows in each image point to the location of the event used as a target in the target-oriented migrations. The yellow arrow points to the location of a fault that is better resolved in (b).
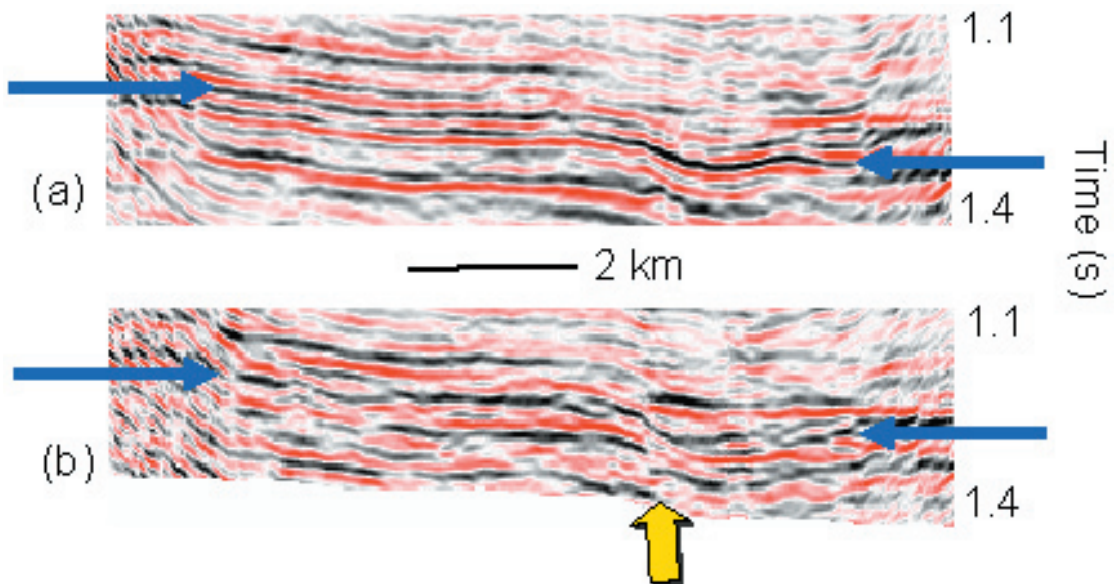
Figure. 5. Comparison between images from the conventional and the target oriented migration. Images stacked in the far-offset range. Once again the fault pointed-to by the yellow arrow is better resolved in the target-oriented image.
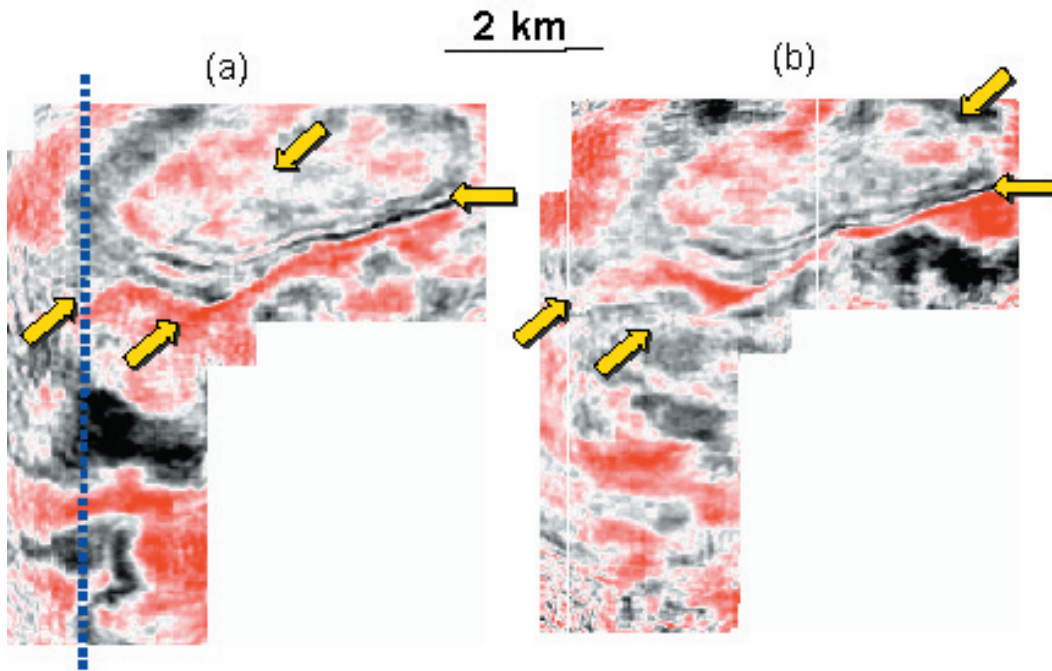
Figure. 6. Comparison of time slices on the full offset range for the: (a) conventional and (b) target oriented migrations. Slice is taken at 1.2 seconds, approximately the time of the target horizon. Faults trending to the NE can be identified between the yellow arrows in each image.
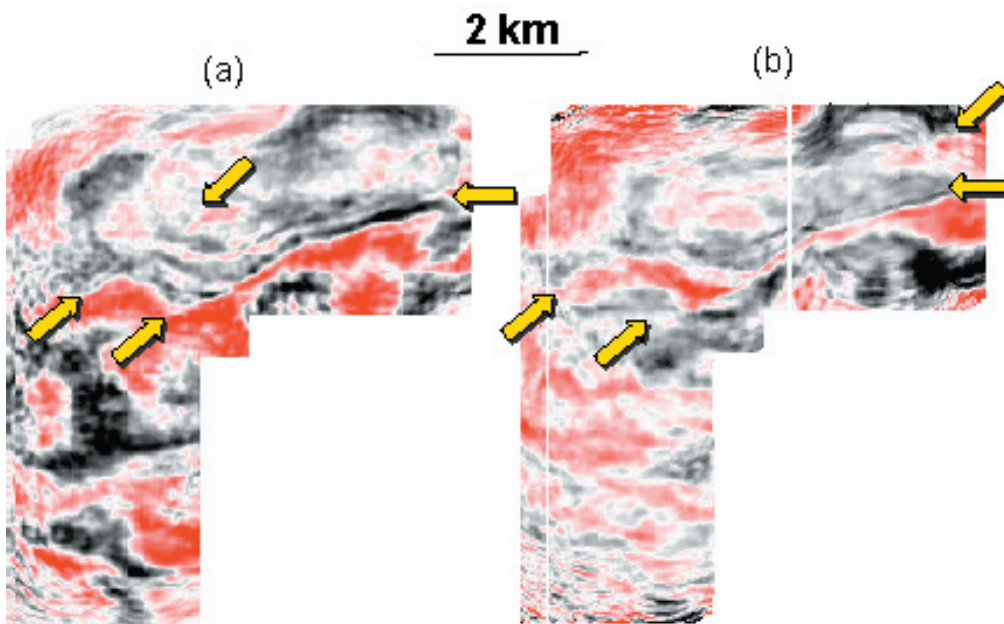

Figure. 7. Comparison of time slices on the far-offset range for the: (a) conventional and (b) target oriented migrations. Time of the slice is 1.2 seconds.
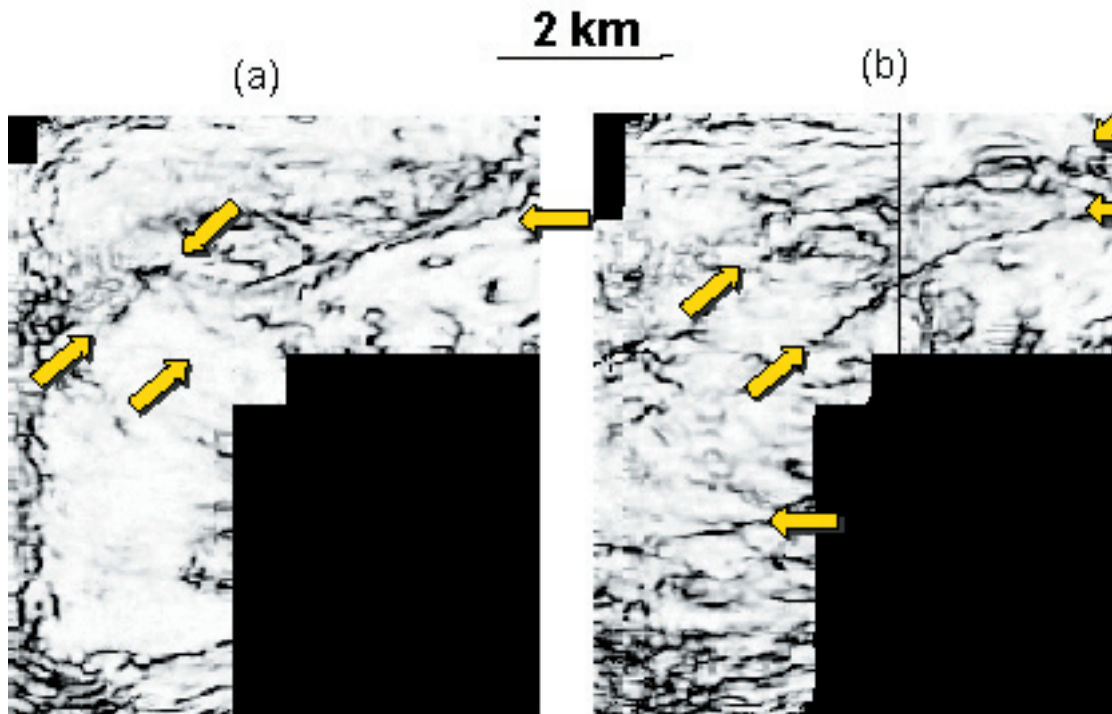
Figure. 8. Comparison between principal component coherence images in the far-offset range stack for the: (a) conventional and (b) target oriented migrations. Time of the slice is 1.2 seconds.

set data for AVO studies, which evolved into a related but different implementation (Hilterman and VanSchuyver, 2003). The next sections will describe the application of the horizon-oriented migration to the imaging of a field dataset from the Fort Worth Basin, Texas, USA. As previously stated, this paper focuses on the impact of the improved frequency content from far-offset imaged data, on image quality, and on lateral and vertical resolution.

DATA PROCESSING

Data was processed twice, initially with a conventional pre-stack time migration and then, with the horizon-oriented stretch-free implementation. The conventional migration work-flow included a migration velocity estimation step. The same velocity field was used for the conventional migration and the horizon-oriented migration. As appropriate for time migration, velocities were computed using a "Deregowski-loop" approach where an initial migration was performed with the same velocities used for NMO correction in

earlier time processing. Using this velocity field, NMO was restored on selected gathers and an additional step of conventional hyperbolic moveout analysis yielded updated velocities, used for the final migration. As a target for the horizon-oriented migration, a horizon interpreted on the stack of the conventional pre-stack migrated data was used as corresponding to the top of one of the major formations of interest in the area. As seen in Figures 4 and 5 this horizon runs roughly between 1.1 and 1.2 seconds; the size of the data block window was 200 ms, centered on the time in the input trace corresponding to the horizon picked time.

Figure 3 compares the results of the two imaging approaches. In the conventional migration, stretch shows up at the longer offsets, and it is notably stronger at the shallower times (i.e., where reflection angle is relatively large). In contrast, the target-oriented migrated data is stretch-free with nicely aligned reflections for the full range of offsets. At the longer offsets, however, crossing events from earlier and later times interfere

with proper imaging of the target events.

VERTICAL RESOLUTION

For the analysis the data was divided in three offset ranges: 0-4000 ft, 4000 – 8000 ft and 8000 – 12500 ft, corresponding to near, middle and far offset ranges. The absolute maximum offset present in the data was around 25000 ft but on average the maximum offset was closer to 15000 ft. The depth of the target horizon lies in the 7000 to 8000 ft range.

Figures 4 and 5 compare stacked images from the full and far offset ranges for the two migrated datasets. It can be observed that for the full-range stack the target-oriented migration image is better resolved than the conventional migration. In the far-offset range images in Figure 5, the target horizon and the fault zone are more sharply defined by the target-oriented migration. This should be attributed to the combined effect of improved frequency content on the far offsets and increased fold of stack available to the target-oriented images. Notice that because of the lower fold, the offset-limited images are of inferior quality compared to those with the full range of offsets. Besides, the target-oriented migration images are slightly noisier and more impacted by migration artifacts than the conventional migration images. This is explained because for this dataset, the signal-to-noise ratio is poorer (Figure 3) and fold distribution is less uniform in the extended offset range included in the far-offset target-oriented migration.

In the very-long offsets (beyond 12500 ft) in the horizon-oriented migration, overcorrected events from the later times in the imaged data window interfere with properly aligned data from earlier times (Figure 3). Failure to image the data at the very-long offsets is a limitation of the hyperbolic moveout assumption implicit in conventional prestack time migration. Inclusion of the overcorrected, not properly imaged events in the stack, results in a distorted and defocused stacked image. Avoiding major distortion in the images is the main reason to limit the offsets from the horizon-oriented migrated data to a maximum of 12500 ft, as described above. Reduction of the offset range is a drastic and suboptimal solution.

A better approach should consider non-hyperbolic moveout in the computation of the operator for the horizon-oriented migration. For the conventional migration, imaging of long-offset data is simply not attempted and, as observed in Figure 3, it is severely distorted by the migration. As usual, this data was muted prior to stacking to obtain stacked images from the conventionally migrated data.

LATERAL RESOLUTION

An improved lateral resolution is fully achieved from the target-oriented migration (Figures 6 and 7). Just as for the vertical images, the pick-corrected migration is comparatively much less resolved and is not shown. In those Figures, the NE-trending faults, indicated by the arrows, are more sharply defined in the target-oriented images for both the far-offset and full offset ranges. Though subtle, definition of features like these is potentially very important for the exploration goals in the survey area.

A final comparison is made in Figure 8 between the conventional and target-oriented migrations at the far-offset range, this time using principal-component coherence. Principal-component coherence (Gersztenkorn and Marfurt, 1999) is a multitrace attribute that provides an image of lateral changes in waveform by computing the similarity between neighboring traces in a 3D data volume. Multitrace attributes such as coherence may reveal subtle geologic features that are lost in conventional images. These attributes are used as a way to assess the lateral resolution in the migrated images generated in this paper. The NE trending faults and other features pointed to by the arrows, are once again better defined by the target-oriented migration (Figure 8).

CONCLUSIONS

A block-moveout, horizon-oriented implementation of Kirchhoff pre-stack migration effectively delivers stretch-free pre-stack imaged data. Imaged data is augmented by long offsets that are discarded by conventional imaging algorithms. This contributes to an improved image quality and larger vertical and lateral resolution. Fully achieving the potential of this technique requires

that non-hyperbolic moveout is properly accounted for in the migration.

The possibility to apply it in a target-oriented fashion has been repeatedly mentioned as one of the strengths of Kirchhoff migration. As shown by others before, and reinforced here, if the target is a horizon, Kirchhoff migration can be implemented so that it is also stretch-free. This imaging approach provides an increased fold of imaged far-offset data with improved frequency content. This impacts image quality and resolution. In the application of this approach to a 3D dataset from the Fort Worth basin, good results have been achieved in imaging subtle fault features that are nevertheless important for the exploration targets in the area.

Finally, moving further in the long-offset range of what is conventionally available, opens up a whole can of worms of new issues that have been swept under the rug or discarded by harsh muting in the conventional approach.

ACKNOWLEDGMENTS

REFERENCES

Barnes, A. E. (1992). Another look at NMO stretch. *Geophysics*. **57**. 749-751.

Brouwer, J. H. (2002). Improved NMO correction with a specific application to shallow-seismic data. *Geophysical Prospecting*. **50**. 225–237.

Castoro, A., White, R. E., and Thomas, R. (2001). Thin-bed AVO: Compensating for the effects of NMO on reflectivity sequences. *Geophysics*. **66**. 1714-1720.

Dong, W. (1999). AVO detectability against tuning and stretching artifacts. *Geophysics*. **64**. 494-503.

Dunkin, J. W. and Levin, F. K. (1973). Effect of normal moveout on a seismic pulse: *Geophysics*. **28**. 635–642.

Gersztenkorn, A. and Marfurt, K. J. (1999). Eigenstructure based coherence computations as an aid to 3D structural and stratigraphic mapping. *Geophysics*. **64**. 1468-1479.

Hilterman, F. (2004). Personal communication.

Hilterman, F. and Van Schuyver, C. (2003). Seismic wide-angle processing to avoid NMO stretch. 73rd Annual International Meeting: Society of Exploration Geophysicists, Expanded Abstracts. 215-218.

Lazaratos, S. and Finn, C. (2004). Deterministic spectral balancing for high-fidelity AVO. 74th Annual International Meeting, Society of Exploration Geophysicists, Expanded Abstracts. 219–223.

Levin, S. A. (1998). Resolution in seismic imaging: Is it all a matter of perspective? *Geophysics*. **63**. 743-749.

Rupert, G. B. and Chun, J. H. (1975). The block move sum normal moveout correction. *Geophysics*. **40**. 17–24.

Shatilo, A. and Aminzadeh, F. (2000). Constant normal-moveout (CNMO) correction. A technique and test results. *Geophysical Prospecting*. **48**. 473-488.

Swan, H. W. (1997). Removal of offset-dependent tuning in AVO analysis. 67th Annual International Meeting, Society of Exploration Geophysicists, Expanded Abstracts. 175–178.

Trickett, S. (2003). Stretch-free stacking. 73rd Annual International Meeting, Society of Exploration Geophysicists, Expanded Abstracts. 2008-2011

Wyatt, K. D., Valasek, P. A., Wyatt, S. B., and Heaton, R. M. (1997). Velocity and illumination studies from horizon−based PSDM, 67th Annual International Meeting: Society of Exploration Geophysicists, Expanded Abstracts, 1801−1804.

Yu, Z., McMechan, G. A., Anno, P. D., and Ferguson, J. F. (2004). Wavelet transform-based prestack multiscale Kirchhoff migration. *Geophysics*. **69**. 1505-1512.